JAN 2 1 1981

Item 83-14 E

NAS 1.60:1794

ORIGINAL

NASA Technical Paper 1794

Chemical Kinetic Models for Combustion of Hydrocarbons and Formation of Nitric Oxide

Casimir J. Jachimowski and Charles H. Wilson

DECEMBER 1980

NASA

NASA Technical Paper 1794

Chemical Kinetic Models for Combustion of Hydrocarbons and Formation of Nitric Oxide

Casimir J. Jachimowski and Charles H. Wilson
Langley Research Center
Hampton, Virginia

National Aeronautics
and Space Administration

**Scientific and Technical
Information Branch**

1980

SUMMARY

The formation of nitrogen oxides (NO_x) during combustion of methane, propane, and a jet fuel, JP-4, was investigated in a jet-stirred combustor. The results of the experiments were interpreted using reaction models in which the nitric oxide (NO) forming reactions were coupled to the appropriate hydrocarbon combustion reaction mechanisms. Comparison between the experimental data and the model predictions reveals that the CH + N_2 reaction process has a significant effect on nitric oxide formation especially in stoichiometric and fuel-rich mixtures. Reaction models were assembled that predicted nitric oxide levels that were in reasonable agreement with the jet-stirred combustor data and with data obtained from a high-pressure (5.9 atm (0.6 MPa)), prevaporized, premixed, flame-tube-type combustor. The results of the experiments and the theoretical studies also suggested that the behavior of hydrocarbon mixtures, like JP-4, may not be significantly different from that of pure hydrocarbons. Application of the propane combustion and nitric oxide formation model to the analysis of NO_x emission data reported for various aircraft gas turbines showed the contribution of the various nitric oxide forming processes to the total NO_x formed.

INTRODUCTION

The ability to describe the kinetics of nitrogen oxide formation during combustion of hydrocarbon-based fuels is an important requirement for the development of analytical combustor models such as those for gas turbines. The mechanism of nitric oxide formation from atmospheric nitrogen has been studied extensively, and during combustion of fuel-lean and near-stoichiometric fuel-air mixtures, the formation of nitric oxide is generally understood by what is often called the extended Zeldovich reaction mechanism:

$$O + N_2 \rightarrow NO + N$$

$$N + O_2 \rightarrow NO + O$$

$$N + OH \rightarrow NO + H$$

This mechanism, when coupled with reactions that describe the oxidation of hydrocarbon species and the formation of atomic oxygen and the hydroxyl radical, predicts nitric oxide production rates and concentrations that are a function of both temperature and equivalence ratio. However, these predictions have not always been in agreement with observed nitric oxide levels, particularly for hydrocarbon-air flames. For example, during an investigation of the formation of nitrogen oxides in hydrogen, carbon monoxide, and propane flames within a jet-stirred combustor, Engleman et al. (ref. 1) compared experimental nitric oxide concentrations with those predicted from a chemical kinetic model of the

appropriate system. The extended Zeldovich mechanism adequately modeled formation of nitric oxide in the nonhydrocarbon (H_2 and CO) systems at all equivalence ratios. However, in the propane flames, the observed levels were significantly underestimated. More recently, Engleman et al. (ref. 2) and Wakelyn et al. (ref. 3) reported similar differences between observed and theoretical nitric oxide levels when the extended Zeldovich reaction scheme is the only path for nitric oxide formation.

Explanations have been proposed to account for these differences between observed and predicted nitric oxide levels in hydrocarbon-air flames. It has been suggested (refs. 4 to 6) that excess amounts ("super-equilibrium") of atomic oxygen and the hydroxyl radical are responsible for the higher observed nitric oxide levels and that the current hydrocarbon oxidation mechanisms do not adequately predict these O and OH concentrations. Malte et al. (ref. 7), however, measured hydroxyl radical and atomic oxygen concentrations formed during combustion of methane in a jet-stirred combustor and found that these concentrations were not high enough to account for the observed NO concentrations. They concluded that the lack of agreement between experiment and theory indicates a possible influence of reactions between hydrocarbon fragments and molecular nitrogen leading to nitric oxide, as first suggested by Fenimore (ref. 8).

Fenimore proposed that the reaction between the CH radical and molecular nitrogen

$$CH + N_2 \rightarrow HCN + N$$

produced intermediates that were subsequently oxidized to nitric oxide. Subsequent experimental studies (refs. 9 to 11) have verified the presence of HCN in various hydrocarbon-air flames. Thus, the oxidation of HCN and N could be a significant source of NO in flames. Engleman et al. (ref. 2) and Wakelyn et al. (ref. 3) have had some success in predicting the NO levels observed during combustion of methane and propane in a jet-stirred combustor. The agreement between observed and calculated NO levels was reached by adjusting the rate coefficient for the reaction $CH + N_2 \rightarrow HCN + N$. The resulting rate coefficients were different for the two studies and furthermore were not in good agreement with the recent rate coefficient expressions reported by Matsui and Nomaguchi (ref. 12) and Blauwens et al. (ref. 13).

The objective of the study reported here was to experimentally and theoretically investigate the production of nitrogen oxides during combustion of various hydrocarbon fuels, including a jet fuel, and attempt to assemble a chemical kinetic combustion and nitric oxide formation model that is consistent with experimental results and recent kinetic data. The experiments were performed in a jet-stirred combustor and the fuels studied were methane, propane, and the jet fuel, JP-4, at fuel-air equivalence ratios from 0.7 to 1.4. Since propane is often used as a surrogate jet fuel in many combustion experiments, a propane-air experiment was carried out under the same test conditions as the jet-fuel-air experiments to provide a direct comparison of the NO levels at identical mass loadings. Such a comparison should indicate whether a propane combustion and NO formation model would also be a good surrogate model for a jet fuel.

EXPERIMENTAL APPARATUS AND PROCEDURE

The combustion device used in these studies consisted of a jet-stirred combustor identical to the device described by Wakelyn et al. (ref. 3) with the exception that the injector, as well as the shell, was made of castable zirconia (see fig. 1). Mixtures of fuel and air were fed to a hemispherical injector

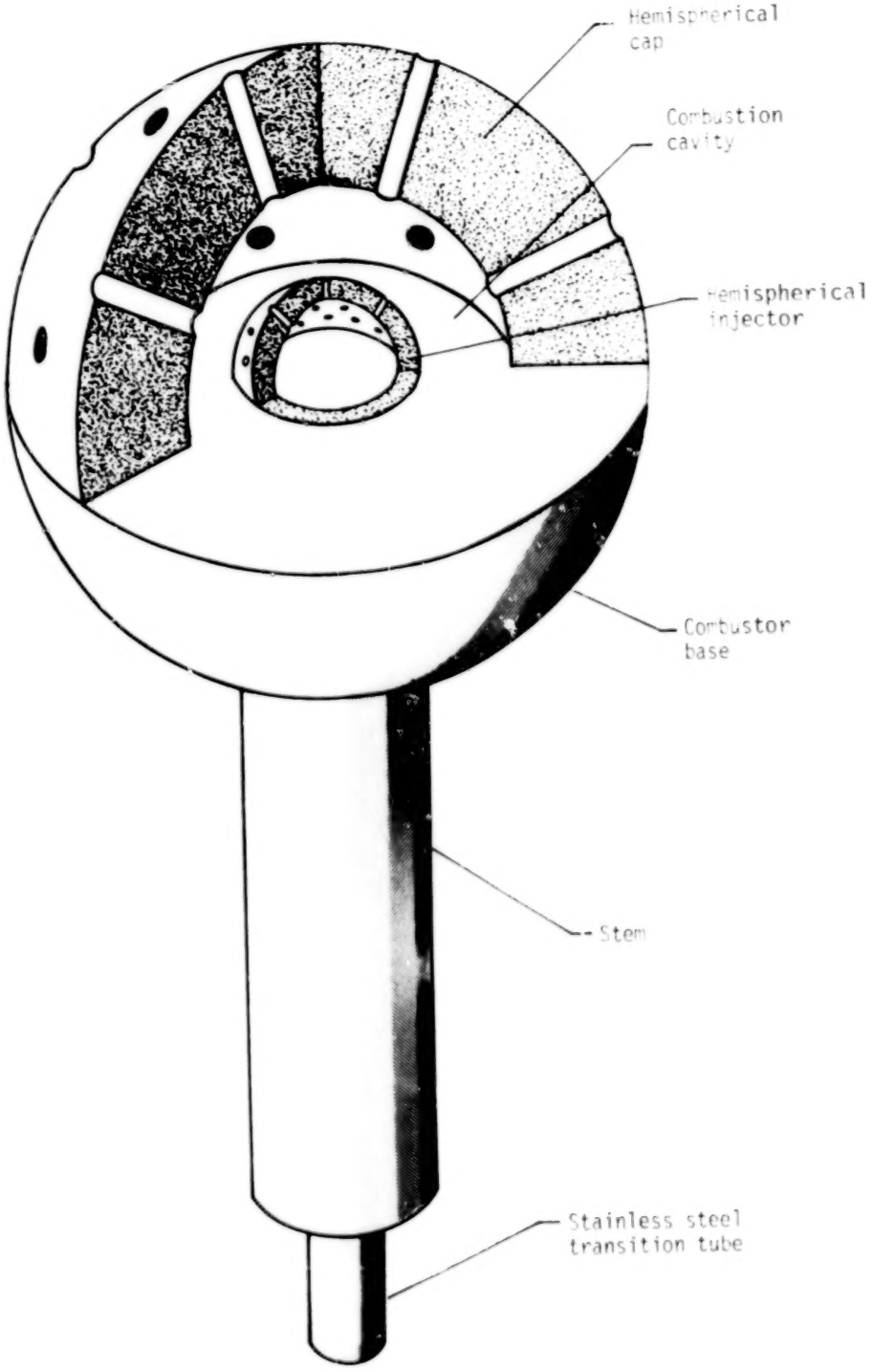

Figure 1.- Cast zirconia jet-stirred combustor.

containing 40 evenly distributed holes of 0.051-cm diameter that opened into a hemispherical combustion cavity of 12.7-cm^3 volume. Combustion products were exhausted through 25 holes of 0.318-cm diameter that were evenly distributed over the hemispherical cap of the combustor. Two additional holes of 0.416-cm diameter were provided in the cap for use as gas sampling and thermocouple ports; these holes were positioned on opposite sides of the cap along a horizontal line located sufficiently above the injector surface to permit probes to pass over the injector without interference.

The change to an all-zirconia combustor design served to avert flashback during combustion of liquid hydrocarbon fuels. The former design, with an inconel injector, allowed sufficient heat to be transferred through the injector wall to raise the temperature of the air-fuel mixture within the injector to its autoignition point, resulting in combustion within the injector itself. This condition could not be avoided for fuel-air equivalence ratios from 0.9 to 1.2 without resorting to intentional cooling of the combustion zone (e.g., Singh (ref. 14) employed a nitrogen diluent). Zirconia provided sufficient resistance to heat transfer across the injector wall to prevent flashback.

The combustion of liquid fuels in this device required a different approach for premixing and metering fuel and air than that described in reference 3 for propane. Since experimental limitations did not readily allow the use of heat alone to effect fuel evaporation, the approach taken by Wright (ref. 15) was followed in which the fuel was both heated and atomized. In the present work, the fuel was finely atomized at approximately 190°C. It was expected that this technique would suffice for JP-4 provided that atomization occurred sufficiently near the combustor injector to prevent condensation of the high-boiling-point fractions of the fuel at temperature below the 100-percent evaporation point. This expectation appeared to be supported by the calculations of reference 16, which indicate that no residue from an average refinery run of JP-4 would be lost through condensation. Results of subsequent experiments with this test configuration confirmed these calculations, since no high-boiling-point fractions could be observed inside the test apparatus after more than 20 liters of JP-4 had passed through the system during the combustion experiments.

The apparatus used to vaporize the fuel and control the flow of fuel-air mixtures into the combustor is depicted in figure 2. Fuel reservoirs consisted of closed vessels pressurized with nitrogen gas. Fuel flow rate was measured by rotameters and controlled by fine-metering valves. Valves located downstream of the rotameters kept sufficient pressure on the fuel to avoid bubble formation from dissolved nitrogen as it passed through the rotameters. Mixtures of different fuels could be obtained by adjusting flow rates from individual fuel reservoirs.

It was found that changes in room temperature could change fuel density and viscosity sufficiently to cause flow rate errors of as much as 1 percent per degree Celsius. Since room temperature ranged from 18°C to 27°C, a controlled temperature water bath was employed to keep fuel passing through the rotameters at a temperature of 40°C ± 0.5°C.

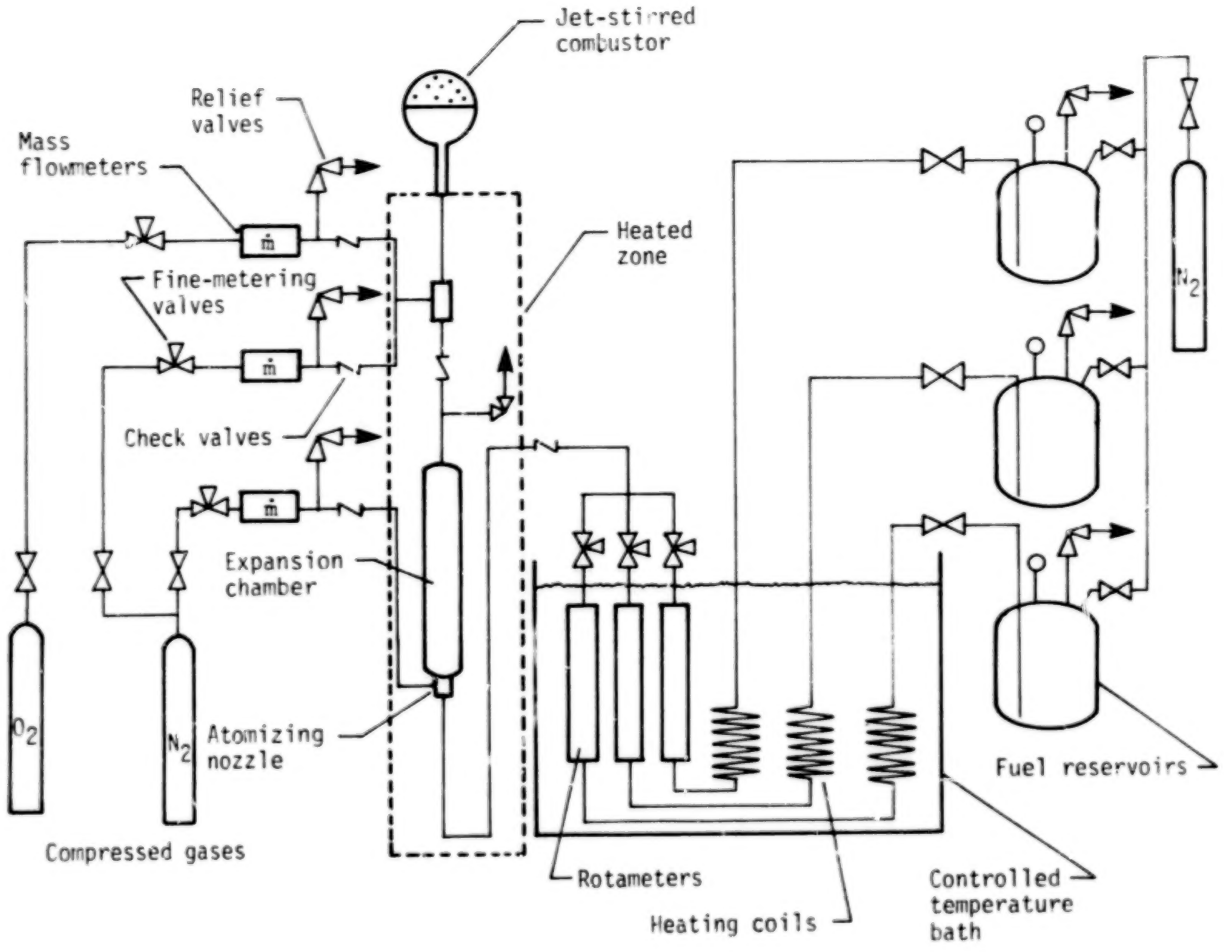

Figure 2.- Schematic diagram of combustor fuel and air supply system.

An internal-mix, two-fluid nozzle was used for atomization in which the flow rate of impinging nitrogen gas was maintained at a constant 20 L/min. This provided fine atomization over the entire range of fuel flows, 0.5 mL/min to 7.5 mL/min. Care was taken in the nozzle design, and in the orientation of the expansion chamber into which the spray was directed, to prevent fuel from dripping because this invariably resulted in unstable combustion.

Downstream of the expansion chamber, oxygen and nitrogen were mixed with the fuel-vapor-nitrogen mixture exiting from the expansion chamber. Flow rates of oxygen and nitrogen were controlled by fine-metering valves and monitored by mass flowmeters. Total oxygen flow rates ranged to 13 L/min and total nitrogen flow rates ranged to 50 L/min. Preheat temperature of the entire combustible fuel-air mixture was measured within the combustor stem with a platinum/platinum+14-percent-rhodium thermocouple at a point sufficiently distant from the combustion cavity to avoid temperature feedback effects from the combustion.

Combustion cavity temperature was measured and gas samples were taken in accordance with the procedures described in reference 3. A traversing iridium/indium+40-percent-rhodium thermocouple measured flame temperature; and a water-cooled, aerodynamically quenched, sampling probe of stainless steel withdrew gas samples for analyses of NO and NO_x with a chemiluminescence analyzer. Gas samples were taken at a probe depth into the combustion cavity of 0.15 to 0.25 cm. The only difference between the sampling procedures in the present work and those described in reference 3 was the sampling dilution ratio: whereas a dilution ratio of 6 to 1 was satisfactory for propane and JP-4, a ratio of approximately 8 to 1 was required for methane combustion to prevent water condensation in the sampling lines.

Experiments were performed at ambient (atmospheric) pressure at a combustor inlet temperature of 27°C (300 K) with the methane-air mixtures, 27°C and 182°C (455 K) with the propane-air mixtures, and 182°C with the JP-4-air mixtures. The combustor mass loadings were between 0.072 and 0.074 g/cm^3-sec corresponding to residence times between 2.4 and 2.6 msec. The fuel-air equivalence ratio was varied between 0.7 and 1.4.

CHEMICAL KINETIC MODELS

The reaction models that were assembled for comparison with the experimental data are, for the most part, based on chemical kinetic and mechanistic information found in the literature. It was not the intent, however, to assemble an extensive list of reactions, but rather to develop reaction mechanisms containing enough detail to describe essential features of the oxidation and nitric oxide formation. The rate coefficients selected for the reactions in the various mechanisms were obtained from the literature whenever possible. (See refs. 3, 10, 12, and 17 to 37.) It must be emphasized at this point that the proposed mechanisms are not necessarily complete since very little kinetic and mechanistic information is available on the hydrocarbon-oxygen systems, especially on reactions involving the lower molecular weight components such as CH and CH_2 that are believed to be important species in the production of nitric oxide in fuel-rich mixtures (ref. 8).

The methane oxidation mechanism that was assembled for this study is listed in table 1. The high-temperature combustion of methane has been investigated for many years, and most of the basic features of the combustion mechanism are known. The methane combustion mechanism used in this study contains, we believe, all these essential features.

The propane combustion mechanism used in this study is listed in table 2. This mechanism is based on the results of an experimental and theoretical study of propane oxidation behind shock waves (ref. 30). The propane combustion mechanism is a rather simplified mechanism in which propane is assumed to rapidly decompose at combustion temperatures and react to form lower molecular weight hydrocarbons such as the methyl radical, ethylene, and acetylene, which are subsequently oxidized. A minimal number of reactions were used to describe the transformation of propane to the lower molecular weight fragments. The mechanism presented in table 2 distinguishes between the normal propyl and isopropyl radicals. This distinction was required to explain the shock tube experiments,

but was unnecessary for the present study. By using an "average" rate coefficient for reactions involving the propyl radical, the propane mechanism can be simplified even further without affecting the calculated nitric oxide levels. The complete propane combustion scheme used in this study consisted of the reactions in table 2 combined with the reactions in table 1.

As noted previously, Fenimore (ref. 8) suggested that the reaction between the CH radical and molecular nitrogen could produce the intermediates HCN and N that eventually were transformed to nitric oxide. The reactions that were selected to describe the transformation of HCN and N to nitric oxide, as well as the formation and consumption of the CH radical, are listed in table 3. Also included in table 3 are reactions describing the formation of NO through N_2O which contributes to NO formation during the combustion of very fuel-lean mixtures. The importance of these reactions in determining nitric oxide levels is discussed later. The reactions listed in table 3 combined with the methane and propane oxidation schemes listed in tables 1 and 2 formed the kinetic models used in this study to calculate nitric oxide levels.

To model the experiments, a computer program was used which describes the jet-stirred combustor as a perfectly stirred reactor (PSR) in steady-state operation. The program is basically a combination of the equilibrium program of Gordon and McBride (ref. 38) and the PSR solution algorithm of Jones and Prothero (ref. 39). Inputs to the program include a reaction mechanism, initial composition, temperature and pressure, and a heat loss parameter to account for the nonadiabatic operation of the reactor. Solutions are provided at desired mass loadings.

RESULTS AND DISCUSSION

Comparison Between Experimental Results and Chemical Kinetic Models

The results of the methane-air, propane-air, and the JP-4-air experiments are plotted in figures 3 to 6 where the measured reaction temperature and nitrogen oxide (NO_x) concentration in parts per million (ppm) are plotted against the fuel-air equivalence ratio. The data were obtained at mass loadings between 0.072 and 0.074 g/cm^3-sec which correspond to residence times between 2.4 and 2.6 msec. Maximum nitrogen oxide concentrations occurred in the range of equivalence ratios between 1.0 to 1.1. The NO_x concentrations and flame temperature for the propane-air and JP-4-air experiments (see figs. 5 and 6) were essentially the same for the stoichiometric and fuel-lean mixtures. For the fuel-rich mixtures, the observed NO_x levels were higher for the jet-fuel experiments; however, as shown later, this can be attributed to higher flame temperatures.

The ability of the proposed mechanisms to predict the experimentally measured nitrogen oxide levels was assessed by simulating the jet-stirred combustor experiments using the PSR program and the reactions and rate coefficients listed in tables 1 to 3. These simulations were made for fuel-air equivalence ratios between 0.8 and 1.3. The heat loss parameter in the PSR program was adjusted to provide a reasonable match between the calculated and measured temperatures for a mass loading of 0.073 g/cm^3-sec. The flame temperatures used in these simulations are noted in figures 3 to 6.

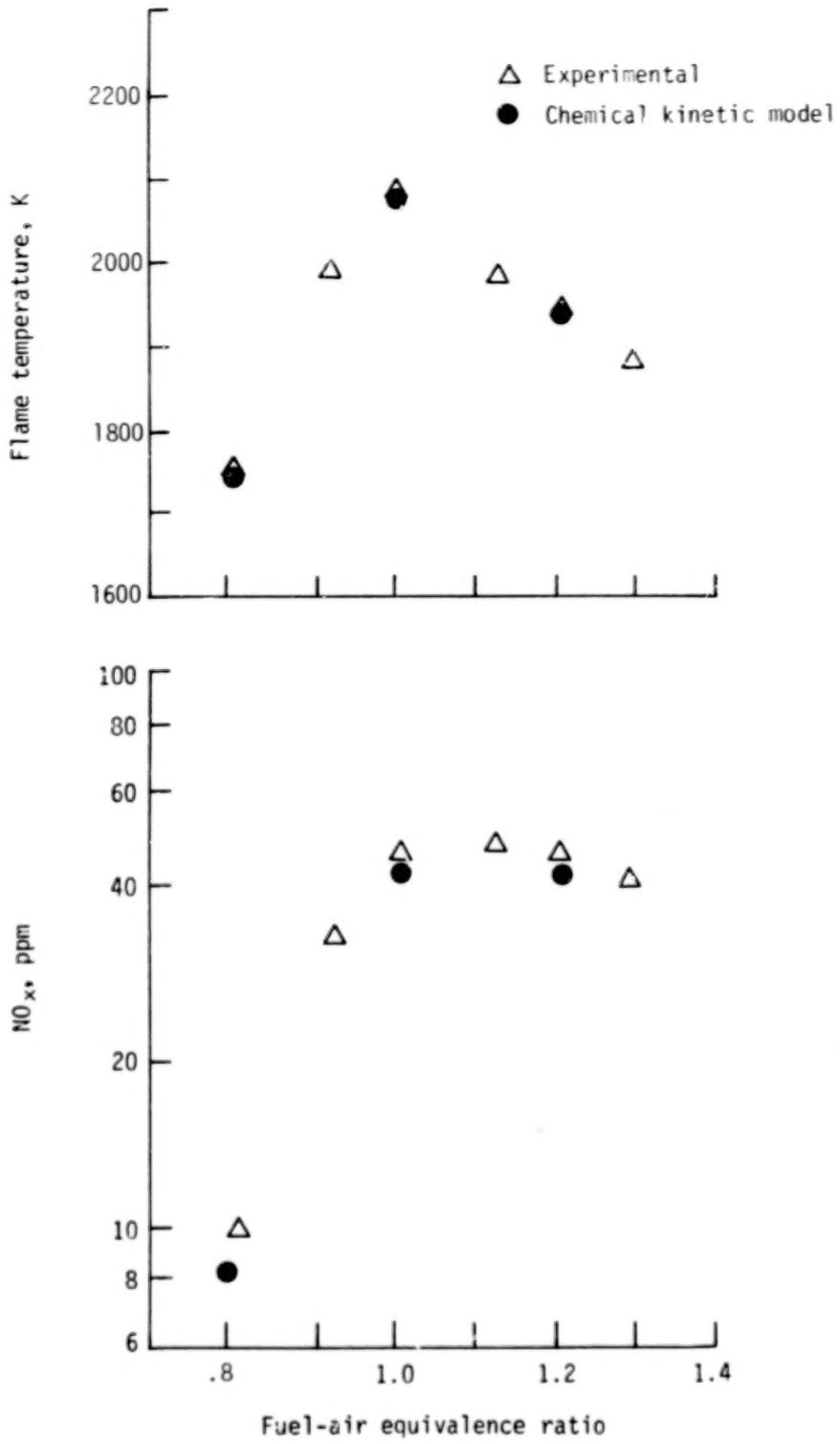

Figure 3.- Experimental and calculated results for methane-air mixtures with combustor inlet temperature of 300 K. Calculations made with $k_{66} = 8 \times 10^{10} \exp(-6844/T)$.

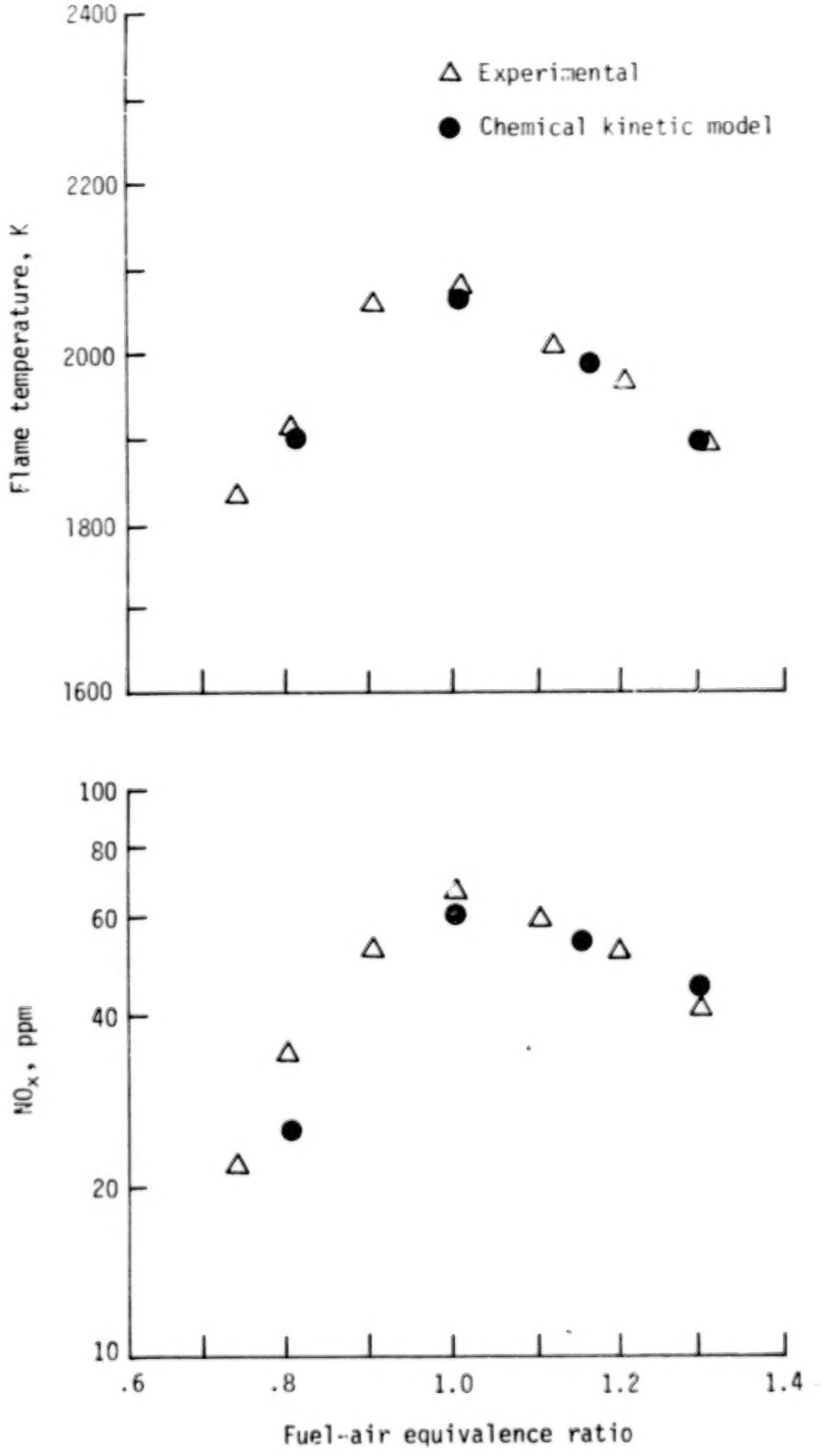

Figure 4.- Experimental and calculated results for propane-air mixtures with combustor inlet temperature of 300 K. Calculations made with $k_{66} = 8 \times 10^{10} \exp(-6844/T)$.

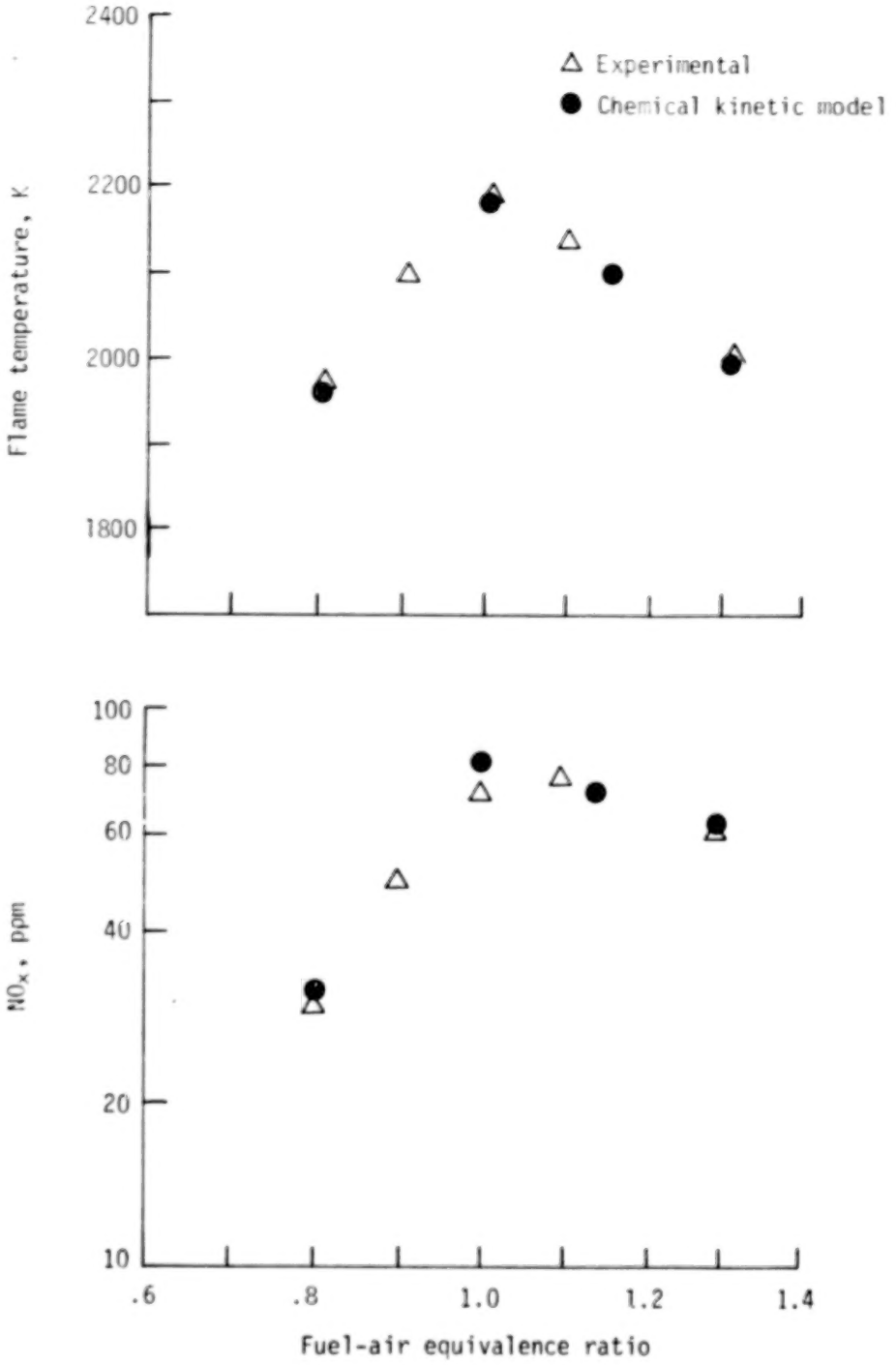

Figure 5.- Experimental and calculated results for propane-air mixtures with combustor inlet temperature of 455 K. Calculations made with $k_{66} = 8 \times 10^{10} \exp(-6844/T)$.

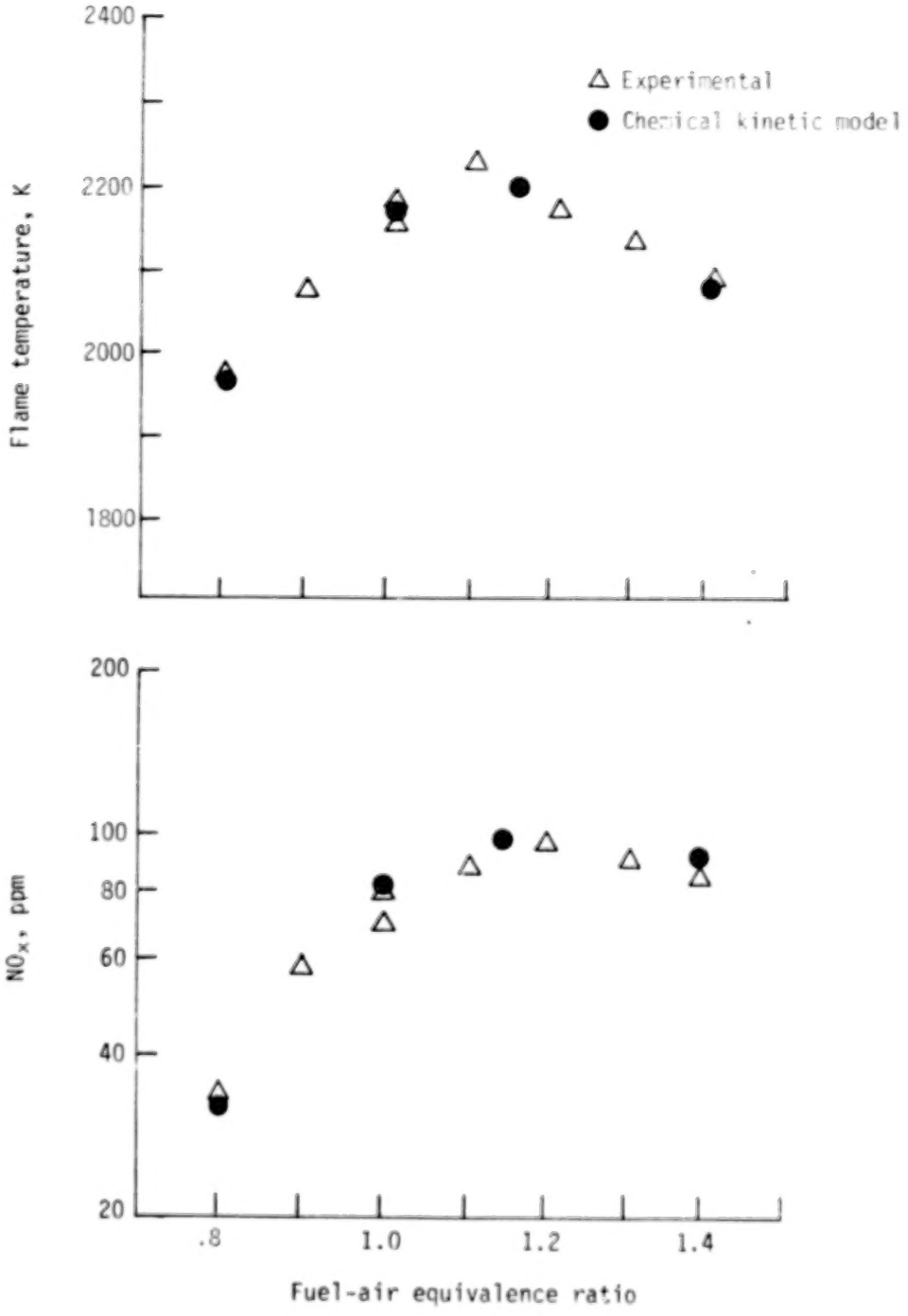

Figure 6.- Experimental and calculated results for JP-4-air mixtures with combustor inlet temperature of 455 K. Calculations made with propane model with $k_{66} = 8 \times 10^{10} \exp(-6844/T)$.

The results of these simulations revealed that the assembled chemical kinetic models overpredicted the measured nitric oxide levels by a factor of up to 4. To better understand the proposed combustion and nitric oxide formation models in relation to the experimental data, a parametric study was performed in which the rate coefficients for selected reactions were varied and the effect on the nitric oxide levels was noted. Such a study would hopefully identify key reactions which govern the formation of NO and determine whether it was possible to achieve good agreement between experiments and computations by making reasonable adjustments to the model. Selected results from the study are given in table 4 for simulations of the methane experiment and one of the propane experiments (at temperature T of 455 K).

The results of the parametric studies revealed that the reactions which describe the formation of NO through the oxidation of HCN and N are needed in the mechanism to account for the observed NO_x concentrations. When the only path for nitric oxide formation is through the extended Zeldovich reactions, the model underpredicts the observed NO_x levels especially for the stiochiometric and fuel-rich mixtures (see table 4).

The reaction between the CH radical and molecular nitrogen (reaction 66) has the greatest effect on the calculated nitric oxide concentrations, as expected. In fact, by adjusting the rate coefficient for this reaction to $k_{66} = 8 \times 10^{10} \exp(-6844/T)$, the nitric oxide levels predicted by the kinetic models are in excellent agreement with the experimental results. The adjusted rate coefficient expression yields rate coefficients that are considerably smaller than the values obtained from the expressions reported in references 12 and 13. The rate coefficient reported in reference 12, $k_{66} = 4 \times 10^{11} \exp(-6844/T)$, is a rough estimate based on experimental data obtained at 2500 K, and the uncertainty associated with this estimate was not reported. The rate coefficient reported in reference 13, $k_{66} = 8 \times 10^{11} \exp(-5536/T)$, represents, according to the investigators, an upper limit with an uncertainty of at least a factor of 2. On the basis of this information, it is difficult to determine whether the adjusted rate coefficient is in reasonable agreement with these expressions. However, the adjusted rate coefficient expression is reasonable for a biomolecular reaction of the type represented by reaction (66). Furthermore, the expression is in fair agreement with a theoretically calculated expression (ref. 2), $k_{66} = 1 \times 10^{11} \exp(-9562/T)$, and the expression, $k_{66} = 1.5 \times 10^{11} \exp(-9562/T)$, reported in reference 3.

As the results presented in table 4 indicate, the other reactions that had a large influence on the calculated NO levels were those that controlled the formation and destruction of the CH radical. In the methane combustion model, the major sources of the CH radical are reactions (59), (60), and (61) with some contribution from reaction (23) for fuel-rich mixtures (equivalence ratios ϕ of approximately 1.3):

(59) $CH_2 + H \rightarrow CH + H_2$

(60) $CH_2 + O \rightarrow CH + OH$

(61) $CH_2 + OH \rightarrow CH + H_2O$

(23) $C_2H + O \rightarrow CH + CO$

The major paths for CH destruction are reactions (25) and (62) with some influence of reactions (63) and (64) for very rich mixtures ($\phi \approx 1.3$):

(25) $CH + O_2 \rightarrow HCO + O$

(62) $CH + CO_2 \rightarrow HCO + CO$

(63) $CH + H \rightarrow C + H_2$

(64) $CH + OH \rightarrow C + H_2O$

Reaction (25) has a large effect for fuel-lean and near-stoichiometric mixtures, while reaction (62) has a large effect over the entire range of equivalence ratios examined.

In the propane combustion model, the major sources of the CH radical are again reactions (59), (60), and (61), with a much greater influence by reaction (23) than in the methane oxidation scheme. The increased effect of reaction (23) occurs because a primary path in the propane oxidation mechanism is the formation of acetylene which is the source of the C_2H radical, while in the methane oxidation mechanism, oxidation of the methyl radical is the primary path. Acetylene is produced in the methane mechanism only after the formation of C_2H_6. The major paths for CH destruction in the propane model are reactions (25) and (62).

As note previously, an objective of the parametric study was to determine whether good agreement between experimental results and the kinetic models could be achieved by making "reasonable" adjustments to the rate coefficients for key reactions. The adjustments were focused mainly on the reactions which controlled the formation and destruction of the CH radical. Since the assembled chemical kinetic models over-predicted the observed NO_x concentrations, a decrease in the nitric oxide levels could be produced by decreasing the rate of production of the CH radical and/or increasing its rate of consumption. As noted previously, the primary sources of the CH radical are different for the methane and propane models. In the methane mechanism, the rate of reaction (61) has the largest influence on CH production, while in the propane model, the rate of reactions (61) and (23) control the formation of CH. Attempts to decrease the rate coefficients of these reactions to achieve reasonable agreement between the calculated and experimental results were not very successful. While reasonable agreement could be achieved separately for either the methane or the propane results, a satisfactory fit to both simultaneously could not be obtained.

Variations in the rate coefficients of the CH consuming reactions revealed that the rate of reaction (62) had a significant effect on calculated NO levels at all equivalence ratios, while reactions (25), (63), and (64) had largest

effects for stoichiometric and fuel-lean mixtures. Attempts to achieve agreement between calculated and experimental results by increasing the rate coefficients for reactions (25), (63), and (64), either separately or together, did not prove successful because of the dominant effect of these reactions in the lean and stoichiometric mixtures. For example, when good agreement was obtained in fuel-rich mixtures, the models underpredicted the observed NO levels in the lean and stoichiometric mixtures. Increasing the rate coefficient of reaction (62), however, was more successful. Very good agreement was achieved by adjusting the rate coefficient of reaction (62) to $k_{62} = 1 \times 10^{12} T^{1/2} \exp(-3020/T)$ which is a factor of 100 larger than the initial expression. Such a large adjustment may not be reasonable, however, since the resulting rate coefficient would have a preexponential factor ($1 \times 10^{12} T^{1/2}$) that is unusually large for a reaction between molecular species.

In summary, the results of the parametric study revealed that the best agreement between the predictions of the chemical kinetic models and the stirred reactor data for methane and propane was achieved by adjusting the rate coefficient for reaction (62) or reaction (66). Since the predicted nitric oxide levels were most sensitive to the rate of reaction (66) and since the required adjustment to the rate coefficient for reaction (62) was considerable and somewhat unreasonable, it was concluded that the most reasonable and kinetically consistent model was achieved when the rate coefficient for reaction (66) was set to $8 \times 10^{10} \exp(-6844/T)$. The nitric oxide levels (expressed as ppm NO_x) predicted by the methane and propane models using the adjusted rate coefficient for reaction (66) are compared with the experimental results in figures 3 to 6. Note that the predictions from the propane model are also in good agreement with the JP-4 experimental results (fig. 6). Apparently, the difference in the NO_x levels that were observed between the propane and JP-4 experiments can be attributed to the difference in flame temperatures. The good agreement between the predictions of the propane model and the JP-4 experimental results also suggests that the propane combustion and NO formation model can be used as a surrogate kinetic model for a jet fuel.

Comparison Between Chemical Kinetic Models and Other Data

As an additional check of the propane combustion and NO formation model, NO_x concentrations predicted by the model were compared with NO_x emissions reported by Anderson (ref. 40) for premixed, prevaporized propane-air mixtures in the NASA Lewis Research Center 10-cm-diameter flame-tube-type combustor. These experiments were conducted at an inlet temperature of 590 K and a pressure of 5.9 atm (0.6 MPa) with a reference velocity of 23 m/sec. The concentration of NO_x was measured at a point 46 cm downstream of the flameholder for a span of fuel-air equivalence ratios ranging from the lean blowout limit to slightly richer than stoichiometric. The results of these studies, given in figure 7, show the strong dependence on equivalence ratio that can be expected from premixed, prevaporized operation. The nitric oxide levels predicted by the propane model (with the adjusted rate coefficient for reaction (66)) are also presented in figure 7. These calculations were made assuming adiabatic operation (ref. 40). Since the NO_x measurements were made at the combustor centerline, the adiabatic assumption was not unreasonable. The agreement between the

analytical model and the data is quite good. Also shown in figure 7 are the contributions that the extended Zeldovich mechanism, the N_2O reaction mechanism, and the CH + N_2 reaction scheme each make to the total NO_x. The N_2O reactions contributed to the total NO_x levels at equivalence ratios less than 0.7, while

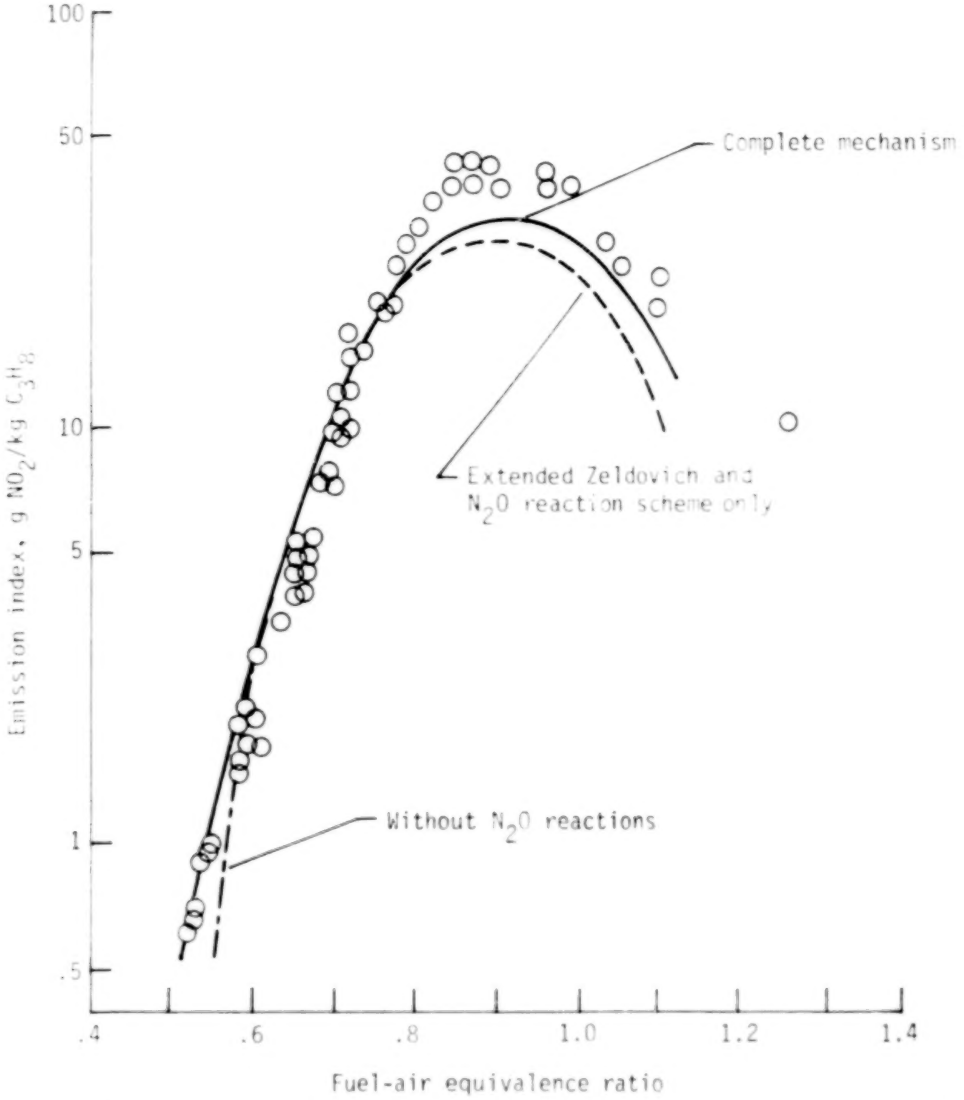

Figure 7.- Experimental NO_x levels for propane-air mixtures in flame-tube-type combustor (ref. 40) compared with NO_x levels predicted by propane combustion and NO formation model.

the oxidation of the HCN and N produced by reaction (66) contributes to the total NO_x when the equivalence ratio is greater than 0.8.

Analysis of Aircraft NO_x Emission Data

Since the propane combustion and nitric oxide formation kinetic model provided a reasonably good description of the JP-4 experimental results, the model was used to investigate the combustion kinetics and the nitric oxide formation

processes for typical aircraft gas turbine operating conditions. This was accomplished by comparing the nitric oxide levels predicted by the model with the NO_x emissions for various aircraft gas turbines as originally presented by Lipfert (ref. 41). Lipfert demonstrated that NO_x emission data, expressed in g NO_2/kg fuel and adjusted to a common humidity level (0.01g H_2O/g dry air), correlated well with combustor inlet temperature for a wide variety of engines. Figure 8 reproduces the Lipfert correlation.

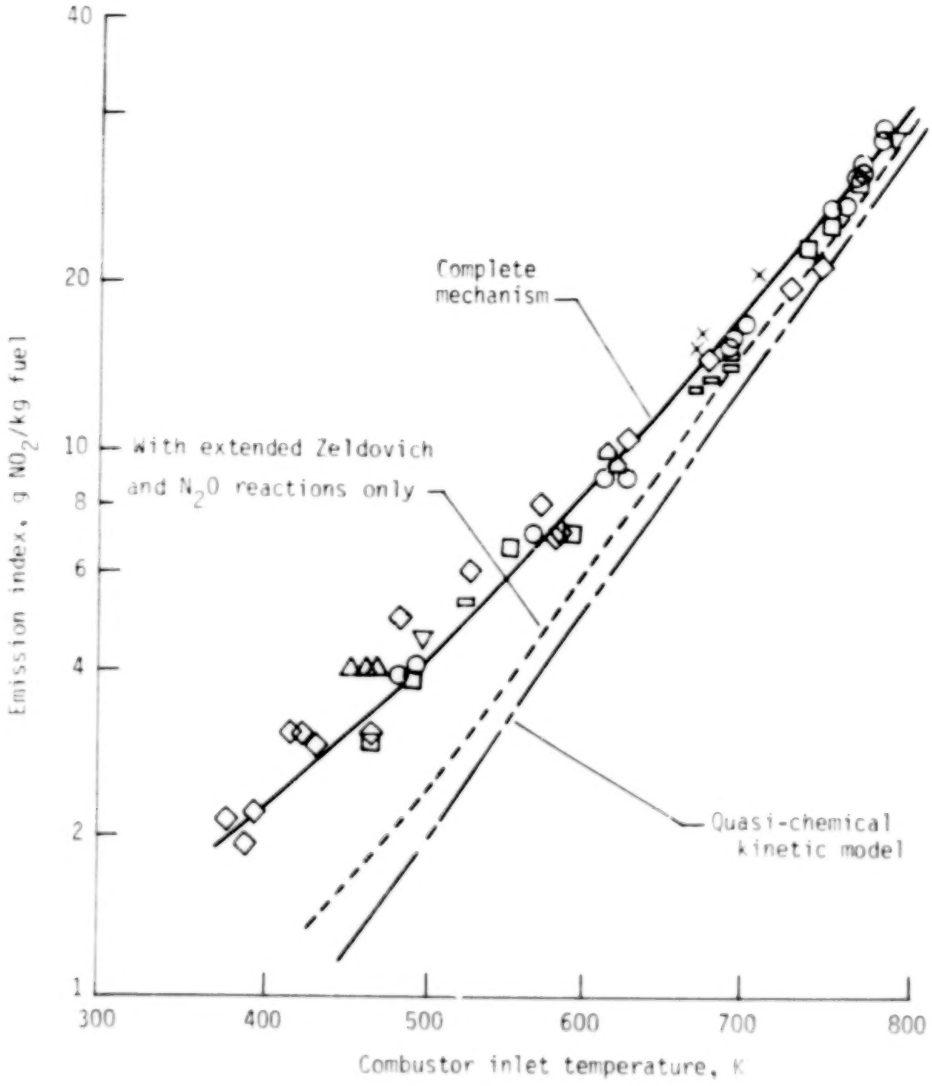

Figure 8.- Comparison of predictions from kinetic models with Lipfert data (ref. 41). In the complete mechanism, $k_{66} = 8 \times 10^{10} \exp(-6844/T)$.

To compare the model with the Lipfert data, it was necessary to determine a representative combustor residence time. The procedure reported by Blazowski et al. (ref. 42) was used to calculate the residence time. Blazowski et al. computed a combustor residence time by comparing the NO_x levels predicted by a model with the Lipfert data for a representative condition - a combustor inlet

temperature of 675 K, a humidity of 0.01g H_2O/g dry air, and an emission index of 15g NO_2/kg fuel. These conditions correspond to sea level static operation at 300 K, a pressure ratio of 13.8, and a representative compressor efficiency of 0.85. Having determined the residence time for this condition, it was assumed to be valid for all other inlet conditions in the Lipfert correlation for a static temperature of 300 K and a compressor efficiency of 0.85.

With these representative operating conditions inserted into the PSR model and adiabatic operation with a stoichiometric fuel-air mixture assumed, the representative combustor residence time was computed to be approximately 0.8 msec. By using this residence time in PSR calculations for the other inlet conditions in the Lipfert correlation, the solid curve shown in figure 8 was generated.

Excellent agreement with the Lipfert data was obtained throughout the entire range of inlet conditions. Also shown in figure 8 are curves representing the NO_x levels predicted by the model when the CH + N_2 reaction scheme is removed and by a quasi-chemical kinetic model. In the quasi-chemical kinetic model, the fuel-oxygen system is assumed to be in chemical equilibrium at the adiabatic flame temperature and the formation of nitric oxide is controlled by the kinetics of the extended Zeldovich reaction scheme. A comparison of the three curves reveals the contribution of several factors to the total NO_x. The difference between the curves generated by the complete model and the model with only the extended Zeldovich and N_2O reaction schemes represents the contribution of the CH + N_2 reaction scheme. This contribution decreases as the temperature increases. The influence of the N_2O reaction scheme on NO_x levels was found to be negligible for the conditions in this analysis.

The difference between the curves generated by the model containing only the extended Zeldovich and N_2O reaction schemes and the quasi-chemical kinetic model represents the contribution of the "super-equilibrium" levels of atomic oxygen and hydroxyl radical to the total NO_x. Blazowski et al. (ref. 42) assembled a model to explain the Lipfert correlation by using a quasi-chemical kinetic model to which they added a "prompt NO" contribution. The results shown in figure 8 indicate that the so-called prompt NO is due to the overshoot of free radical concentrations and the CH + N_2 reactions.

CONCLUDING REMARKS

The objective of this study has been to assemble a chemical kinetic mechanism that can describe the formation of nitric oxide during the combustion of hydrocarbon-based fuels. It was shown that the experimental results could be explained in terms of a reaction mechanism in which the CH + N_2 reaction process has a significant role in the formation of NO expecially in fuel-rich mixtures. The proposed mechanism contains many reactions and rate coefficients that have not been experimentally verified. Therefore, the mechanism may not be unique and further refinements will be required as more kinetic and mechanistic data become available. The proposed mechanisms, however, do not appear unreasonable and the fact that reasonable agreement was achieved between the calculated results and the experimental data for two different hydrocarbons, as well as for data obtained from a different reactor (the Lewis Research Center

prevaporized, premixed flame-tube-type combustor), suggests that the essential features of the nitric oxide formation processes are contained in the model.

Furthermore, the similarity between the NO_x levels produced in the propane and JP-4 experiments, as well as the ability of the propane combustion and nitric oxide formation model to predict the jet-stirred JP-4 results and match the Lipfert aircraft gas turbine data, suggest that the behavior of hydrocarbon mixtures may not be significantly different from the behavior or pure hydrocarbons, such as propane.

Langley Research Center
National Aeronautics and Space Administration
Hampton, VA 23665
December 1, 1980

REFERENCES

1. Engleman, V. S.; Bartok, W.; Longwell, J. P.; and Edelman, R. B.: Experimental and Theoretical Studies of NO_x Formation in a Jet-Stirred Combustor. Fourteenth Symposium (International) on Combustion, Combustion Inst., 1973, pp. 755-765.

2. Engleman, V. S.; Siminski, V. J.; and Bartok, W.: Mechanism and Kinetics of the Formation of NO_x and Other Combustion Pollutants. Phase II. Modified Combustion. EPA-600/7-76-009b, U.S. Environ. Prot. Agency, Aug. 1976. (Available from NTIS as PB-258 875.)

3. Wakelyn, N. T.; Jachimowski, Casimir J.; and Wilson, Charles H.: Experimental and Analytical Study of Nitric Oxide Formation During Combustion of Propane in a Jet-Stirred Combustor. NASA TP-1181, 1978.

4. Bowman, C. T.; and Seery, D. J.: Investigation of NO Formation Kinetics in Combustion Processes: The Methane-Oxygen-Nitrogen Reaction. Emissions From Continuous Combustion Systems, Walter Cornelius and William G. Agnew, eds., Plenum Press, Inc., 1972, pp. 123-139.

5. Bowman, Craig T.: Kinetics of Nitric Oxide Formation in Combustion Processes. Fourteenth Symposium (International) on Combustion, Combustion Inst., 1973, pp. 729-738.

6. Sarofim, A. F.; and Pohl, J. H.: Kinetics of Nitric Oxide Formation in Premixed Laminar Flames. Fourteenth Symposium (International) on Combustion, Combustion Inst., 1973, pp. 739-754.

7. Malte, Philip C.; Schmidt, Stephen C.; and Pratt, David T.: Hydroxyl Radical and Atomic Oxygen Concentrations in High-Intensity Turbulent Combustion. Sixteenth Symposium (International) on Combustion, Combustion Inst., c.1977, pp. 145-155.

8. Fenimore, C. P.: Formation of Nitric Oxide in Premixed Hydrocarbon Flames. Thirteenth Symposium (International) on Combustion, Combustion Inst., c.1971, pp. 373-380.

9. Bachmaier, F.; Eberius, K. H.; and Just, Th.: The Formation of Nitric Oxide and the Detection of HCN in Premixed Hydrocarbon-Air Flames at 1 Atmosphere. Combust. Sci. & Technol., vol. 7, no. 2, 1973, pp. 77-84.

10. Haynes, B. S.; Iverach, D.; and Kirov, N. Y.: The Behavior of Nitrogen Species in Fuel Rich Hydrocarbon Flames. Fifteenth Symposium (International) on Combustion, Combustion Inst., 1974, pp. 1103-1112.

11. Morley, C.: The Formation and Destruction of Hydrogen Cyanide From Atmospheric and Fuel Nitrogen in Rich Atmospheric-Pressure Flame. Combust. & Flame, vol. 27, no. 2, Oct. 1976, pp. 189-204.

12. Matsui, Yasugi; and Nomaguchi, Tamatsu: Spectroscopic Study of Prompt Nitrogen Oxide Formation Mechanism in Hydrocarbon-Air Flames. Combust. & Flame, vol. 32, no. 2, June 1978, pp. 205-214.

13. Blauwens, Joanna; Smets, Bruno; and Peeters, Jozef: Mechanism of "Prompt" NO Formation in Hydrocarbon Flames. Sixteenth Symposium (International) on Combustion, Combustion Inst., c.1977, pp. 1055-1064.

14. Singh, Surendra: A Study of Methanol Combustion and Oxides of Nitrogen Formation in a Jet-Stirred Reactor. Ph. D. Disser., Washington State Univ., 1978.

15. Wright, Franklin J.: The Formation of Carbon Under Well-Stirred Conditions. Twelfth Symposium (International) on Combustion, Combustion Inst., 1969, pp. 867-875.

16. Graves, Charles C.; and Bahr, Donald W.: Atomization and Evaporation of Liquid Fuels. Basic Considerations in the Combustion of Hydrocarbon Fuels with Air, NACA Rep. 1300, 1957, pp. 1-31.

17. Tabayashi, K.; and Bauer, S. H.: The Early Stages of Pyrolysis and Oxidation of Methane. Combust. & Flame, vol. 34, no. 1, Jan. 1979, pp. 63-83.

18. Peeters, Jozef; and Mahnen, Gilbert: Reaction Mechanisms and Rate Constants of Elementary Steps in Methane-Oxygen Flames. Fourteenth Symposium (International) on Combustion, Combustion Inst., 1973, pp. 133-146.

19. Jachimowski, Casimir J.: Kinetics of Oxygen Atom Formation During the Oxidation of Methane Behind Shock Waves. Combust. & Flame, vol. 23, no. 2, Oct. 1974, pp. 233-248.

20. Jensen, D. E.; and Jones, G. A.: Reaction Rate Coefficients for Flame Calculations. Combust. & Flame, vol. 32, no. 1, May 1978, pp. 1-34.

21. Olson, D. B.; and Gardiner, W. C., Jr.: Combustion of Methane in Fuel-Rich Mixtures. Combust. & Flame, vol. 32, no. 2, June 1978, pp. 151-161.

22. Peeters, Jozef; and Mahnen, Gilbert: Structure of Ethylene-Oxygen Flames. Reaction Mechanism and Rate Constants of Elementary Reactions. Combustion Institute European Symposium 1973, F. J. Weinberg, ed., Academic Press, Inc., pp. 53-58.

23. Jachimowski, Casimir J.: An Experimental and Analytical Study of Acetylene and Ethylene Oxidation Behind Shock Waves. Combust. & Flame, vol. 29, no. 1, 1977, pp. 55-66.

24. Shaub, W. M.; and Bauer, S. H.: The Reduction of Nitric Oxide During the Combustion of Hydrocarbons: Methodology for a Rational Mechanism. Combust. & Flame, vol. 32, no. 1, May 1978, pp. 35-55.

25. Tunder, R.; Mayer, S.; Cook, E.; and Schieler, L.: Compilation of Reaction Rate Data for Nonequilibrium Performance and Reentry Calculation Programs. SSD-TR-67-45, U.S. Air Force, Jan. 1967. (Available from DTIC as AD 818 485.)

26. Gardiner, W. C., Jr.; Mallard, W. G.; McFarland, M.; Morinaga, K.; Owen, J. H.; Rawlins, W. T.; Takeyama, T.; and Walker, B. F.: Elementary Reaction Rates From Post-Induction-Period Profiles in Shock-Initiated Combustion. Fourteenth Symposium (International) on Combustion, Combustion Inst., 1973, pp. 61-75.

27. Schott, Garry L.: Further Studies of Exponential Branching Rates in Reflected-Shock Heated, Nonstoichiometric H_2-CO-O_2 Systems. Combust. & Flame, vol. 21, no. 3, Dec. 1973, pp. 357-370.

28. Jenkins, D. R.; Yumlu, V. S.; and Spaulding, D. B.: Combustion of Hydrogen and Oxygen in a Steady-Flow Adiabatic Stirred Reactor. Eleventh Symposium (International) on Combustion, Combust. Inst., 1967, pp. 779-790.

29. Gay, A.; and Pratt, N. H.: Hydrogen-Oxygen Recombination Measurements in a Shock Tube Steady Expansion. Shock Tube Research. Proceedings of the Eighth International Shock Tube Symposium, J. L. Stollery, A. G. Gaydon, and P. R. Owen, eds., Chapman and Hall Ltd., c.1971, pp. 39/1-39/13.

30. McLain, Allen G.; and Jachimowski, Casimir J.: Chemical Kinetic Modeling of Propane Oxidation Behind Shock Waves. NASA TN D-8501, 1977.

31. Albers, E. A.; Hoyermann, K.; Schacke, H.; Schmatjko, K. J.; Wagner, H. Gg.; and Wolfrum, J.: Absolute Rate Coefficients for the Reaction of H-Atoms With N_2O and Some Reactions of CN Radicals. Fifteenth Symposium (International) on Combustion, Combustion Inst., 1974, pp. 765-773.

32. Mayer, S. W.; Schieler, L.; and Johnston, H. S.: Computation of High-Temperature Rate Constants for Biomolecular Reactions of Combustion Products. Eleventh Symposium (International) on Combustion, Combustion Inst., 1967, pp. 837-844.

33. Mulvihill, Juliet N.; and Phillips, Leon F.: Breakdown of Cyanogen in Fuel-Rich $H_2/N_2/O_2$ Flames. Fifteenth Symposium (International) on Combustion, Combustion Inst., 1974, pp. 1113-1122.

34. Baulch, D. L.; Drysdale, D. D.; and Horne, D. G.: Evaluated Kinetic Data for High Temperature Reactions. Volume 2 - Homogeneous Gas Phase Reactions of the H_2-N_2-O_2 System. Butterworth & Co. (Publ.), Ltd., c.1973.

35. Flower, W. L.; Hanson, R. K.; and Kruger, C. H.: Kinetics of the Reaction of Nitric Oxide With Hydrogen. Fifteenth Symposium (International) on Combustion, Combust. Inst., c.1975, pp. 823-832.

36. Benson, S. W.; Golden, D. M; Lawrence, R. W.; Shaw, Robert; and Woolfolk, R. W.: Estimating the Kinetics of Combustion Including Reactions Involving Oxides of Nitrogen and Sulfur. EPA-600/2-75-019, U.S. Environ. Prot. Agency, Aug. 1975.

37. Milks, David; and Matula, Richard A.: A Single-Pulse Shock-Tube Study of the Reaction Between Nitrous Oxide and Carbon Monoxide. Fourteenth Symposium (International) on Combustion, Combustion Inst., 1973, pp. 83-97.

38. Gordon, Sanford; and McBride, Bonnie J.: Computer Program for Calculation of Complex Chemical Equilibrium Compositions, Rocket Performance, Incident and Reflected Shocks, and Chapman-Jouguet Detonations. NASA SP-273, 1971.

39. Jones, A.; and Prothero, A.: The Solution of the Steady-State Equations for an Adiabatic Stirred Reactor. Combust. & Flame, vol. 12, no. 5, Oct. 1968, pp. 457-464.

40. Anderson, David N.: Effect of Premixing on Nitric Oxide Formation. NASA TM X-68220, 1973.

41. Lipfert, F. W.: Correlation of Gas Turbine Emissions Data. Paper 72-GT-60, American Soc. Mech. Eng., Mar. 1972.

42. Blazowski, W. S.; Walsh, D. E.; and Mach, K. D.: Predication of Aircraft Gas Turbine NO_x Emission Dependence on Engine Operating Parameters and Ambient Conditions. AIAA Paper No. 73-1275, Nov. 1973.

TABLE 1.- METHANE OXIDATION SCHEME

Reaction	A (a)	n (a)	C (a)	Ref.
(1) $M + CH_4 \rightarrow CH_3 + H + M$	1.00×10^{17}	0	43 180	17
(2) $H + CH_4 \rightarrow CH_3 + H_2$	7.23×10^{14}	0	7 580	17
(3) $O + CH_4 \rightarrow CH_3 + OH$	4.10×10^{14}	0	7 031	17
(4) $OH + CH_4 \rightarrow CH_3 + H_2O$	3.00×10^{13}	0	3 020	18
(5) $CH_3 + O_2 \rightarrow CH_2O + OH$	1.70×10^{12}	0	7 046	19
(6) $CH_3 + O \rightarrow CH_2O + H$	1.30×10^{14}	0	1 006	18
(7) $CH_3 + CH_3 \rightarrow C_2H_6$	6.00×10^{12}	0	-500	20
(8) $H + C_2H_6 \rightarrow H_2 + C_2H_5$	1.30×10^{14}	0	4 715	21
(9) $O + C_2H_6 \rightarrow OH + C_2H_5$	1.80×10^{13}	0	3 070	21
(10) $OH + C_2H_6 \rightarrow H_2O + C_2H_5$	6.30×10^{13}	0	1 810	21
(11) $H + C_2H_5 \rightarrow 2CH_3$	1.00×10^{13}	0	0	17
(12) $H + C_2H_5 \rightarrow C_2H_4 + H_2$	4.80×10^{13}	0	0	20
(13) $M + C_2H_5 \rightarrow C_2H_4 + H + M$	6.80×10^{17}	0	16 004	17
(14) $H + C_2H_4 \rightarrow C_2H_3 + H_2$	1.10×10^{14}	0	4 279	22
(15) $O + C_2H_4 \rightarrow CH_3 + HCO$	2.50×10^{13}	0	2 516	22
(16) $O + C_2H_4 \rightarrow CH_2 + CH_2O$	2.26×10^{13}	0	1 359	22

[a]The parameters A, n, and C refer to the rate coefficient equation $k = AT^n \exp(-C/T)$. The rate coefficient units are sec^{-1} for unimolecular reactions, $cm^3/mol\text{-}sec$ for bimolecular reactions, and $cm^6/mol^2\text{-}sec$ for termolecular reactions.

TABLE 1.- Continued

Reaction	A (a)	n (a)	C (a)	Ref.
(17) $OH + C_2H_4 \rightarrow C_2H_3 + H_2O$	1.00×10^{14}	0	1 761	23
(18) $M + C_2H_3 \rightarrow C_2H_2 + H + M$	7.94×10^{14}	0	15 853	23
(19) $H + C_2H_2 \rightarrow C_2H + H_2$	7.76	3.2	250	21
(20) $O + C_2H_2 \rightarrow CH_2 + CO$	5.20×10^{13}	0	1 862	23
(21) $OH + C_2H_2 \rightarrow C_2H + H_2O$	6.00×10^{12}	0	3 523	22
(22) $C_2H + O_2 \rightarrow HCO + CO$	1.00×10^{13}	0	3 523	22
(23) $C_2H + O \rightarrow CO + CH$	1.40×10^{13}	0	1 585	24
(24) $CH_2 + O_2 \rightarrow HCO + OH$	1.00×10^{14}	0	1 862	22
(25) $CH + O_2 \rightarrow HCO + O$	1.00×10^{13}	0	0	22
(26) $CH_3 + H \rightarrow CH_2 + H_2$	1.80×10^{13}	.7	1 510	25
(27) $CH_3 + O \rightarrow CH_2 + OH$	1.00×10^{13}	.5	8 556	25
(28) $CH_3 + OH \rightarrow CH_2 + H_2O$	6.00×10^{10}	.7	1 006	25
(29) $H + CH_2O \rightarrow HCO + H_2$	3.00×10^{13}	0	2 100	20
(30) $O + CH_2O \rightarrow HCO + OH$	1.20×10^{14}	0	2 200	20
(31) $OH + CH_2O \rightarrow HCO + H_2O$	6.00×10^{13}	0	500	20
(32) $M + HCO \rightarrow H + CO + M$	5.00×10^{14}	0	9 562	23

[a]The parameters A, n, and C refer to the rate coefficient equation $k = AT^n \exp(-C/T)$. The rate coefficient units are sec^{-1} for unimolecular reactions, $cm^3/mol\text{-}sec$ for bimolecular reactions, and $cm^6/mol^2\text{-}sec$ for termolecular reactions.

TABLE 1.- Concluded

Reaction	A (a)	n (a)	C (a)	Ref.
(33) $H + HCO \rightarrow H_2 + CO$	1.20×10^{14}	0	2 500	20
(34) $O + HCO \rightarrow OH + CO$	1.80×10^{13}	0	2 500	20
(35) $OH + HCO \rightarrow H_2O + CO$	6.00×10^{12}	0	0	20
(36) $OH + CO \rightarrow CO_2 + H$	4.00×10^{12}	0	4 026	26
(37) $CO + O + M \rightarrow CO_2 + M$	2.50×10^{15}	0	2 200	20
(38) $H + O_2 \rightarrow OH + O$	1.22×10^{17}	-.91	8 369	27
(39) $O + H_2 \rightarrow OH + H$	2.07×10^{14}	0	920	27
(40) $OH + H_2 \rightarrow H_2O + H$	5.20×10^{13}	0	3 271	26
(41) $OH + OH \rightarrow H_2O + O$	5.50×10^{13}	0	3 523	26
(42) $H + H + M \rightarrow H_2 + M$				
$M = H_2O$	5.00×10^{18}	-1.15	0	28
M = All others	$\frac{1}{5}$ k(M = H_2O)			29
(43) $H + OH + M \rightarrow H_2O + M$				
$M = H_2O$	2.40×10^{17}	0	-252	28
M = All others	$\frac{1}{6}$ k(M = H_2O)			29
(44) $H + O + M \rightarrow OH + M$	3.60×10^{18}	-1.00	22	20

[a]The parameters A, n, and C refer to the rate coefficient equation $k = AT^n \exp(-C/T)$. The rate coefficient units are sec^{-1} for unimolecular reactions, $cm^3/mol\text{-}sec$ for bimolecular reactions, and $cm^6/mol^2\text{-}sec$ for termolecular reactions.

TABLE 2.- PROPANE REACTION SCHEME

Reaction	A (a)	n (a)	C (a)	Ref.
(45) $M + C_3H_8 \rightarrow CH_3 + C_2H_5 + M$	5.00×10^{15}	0	32 713	3
(46) $CH_3 + C_3H_8 \rightarrow CH_4 + n\text{-}C_3H_7$	2.00×10^{13}	0	5 184	30
(47) $CH_3 + C_3H_8 \rightarrow CH_4 + i\text{-}C_3H_7$	2.00×10^{13}	0	5 184	30
(48) $H + C_3H_8 \rightarrow H_2 + n\text{-}C_3H_7$	6.30×10^{13}	0	4 026	30
(49) $H + C_3H_8 \rightarrow H_2 + i\text{-}C_3H_7$	6.30×10^{13}	0	4 026	30
(50) $O + C_3H_8 \rightarrow OH + n\text{-}C_3H_7$	5.00×10^{13}	0	5 033	30
(51) $O + C_3H_8 \rightarrow OH + i\text{-}C_3H_7$	5.00×10^{13}	0	5 033	30
(52) $OH + C_3H_6 \rightarrow H_2O + n\text{-}C_3H_7$	1.60×10^{14}	0	1 580	30
(53) $OH + C_3H_8 \rightarrow H_2O + i\text{-}C_3H_7$	1.60×10^{14}	0	1 580	30
(54) $n\text{-}C_3H_7 \rightarrow C_2H_4 + CH_3$	4.00×10^{13}	0	16 658	30
(55) $i\text{-}C_3H_7 \rightarrow C_2H_4 + CH_3$	1.00×10^{12}	0	17 363	30
(56) $n\text{-}C_3H_7 \rightarrow C_3H_6 + H$	6.30×10^{13}	0	19 124	30
(57) $i\text{-}C_3H_7 \rightarrow C_3H_6 + H$	2.00×10^{14}	0	20 785	30
(58) $O + C_3H_6 \rightarrow C_2H_4 + CH_2O$	1.00×10^{13}	0	0	30

[a]The parameters A, n, and C refer to the rate coefficient equation $k = AT^n \exp(-C/T)$. The rate coefficient units are sec^{-1} for unimolecular reactions, $cm^3/mol\text{-}sec$ for bimolecular reactions, and $cm^6/mol^2\text{-}sec$ for termolecular reactions.

TABLE 3.- HYDROCARBON FRAGMENT AND NITRIC OXIDE FORMATION REACTION SCHEME

Reaction	A (a)	n (a)	C (a)	Ref.
(59) $CH_2 + H \rightarrow CH + H_2$	2.90×10^{11}	0.70	13 085	25
(60) $CH_2 + O \rightarrow CH + OH$	3.20×10^{11}	.50	13 085	25
(61) $CH_2 + OH \rightarrow CH + H_2O$	5.00×10^{11}	.50	3 020	25
(62) $CH + CO_2 \rightarrow HCO + CO$	1.00×10^{10}	.50	3 020	25
(63) $CH + H \rightarrow C + H_2$	6.40×10^{11}	.70	1 006	25
(64) $CH + OH \rightarrow C + H_2O$	5.00×10^{11}	.50	5 033	25
(65) $C + O_2 \rightarrow CO + O$	5.00×10^{11}	.50	2 013	25
(66) $CH + N_2 \rightarrow HCN + N$	4.00×10^{11} 8.00×10^{10}	0 0	6 844 6 844	12 This study
(67) $CN + H_2 \rightarrow HCN + H$	6.00×10^{13}	0	2 669	31
(68) $O + HCN \rightarrow CN + OH$	1.40×10^{11}	.70	8 505	32
(69) $OH + HCN \rightarrow CN + H_2O$	2.00×10^{11}	.60	2 516	25
(70) $CN + CO_2 \rightarrow NCO + CO$	3.70×10^{12}	0	0	10
(71) $CN + O_2 \rightarrow NCO + O$	3.20×10^{13}	0	505	31
(72) $H + NCO \rightarrow NH + CO$	2.00×10^{13}	0	0	33
(73) $O + NCO \rightarrow NO + CO$	2.00×10^{13}	0	0	33
(74) $N + NCO \rightarrow N_2 + CO$	1.00×10^{13}	0	0	3
(75) $CH + NO \rightarrow N + HCO$	1.00×10^{14}	0	0	24
(76) $CH + NO \rightarrow O + HCN$	1.00×10^{13}	0	0	24

[a]The parameters A, n, and C refer to the rate coefficient equation $k = AT^n \exp(C/T)$. The rate coefficient units are sec^{-1} for unimolecular reactions, cm^3/mol-sec for bimolecular reactions, and cm^6/mol^2-sec for termolecular reactions.

TABLE 3.- Concluded

Reaction	A (a)	n (a)	C (a)	Ref.
(77) $O + N_2 \rightarrow NO + N$	7.60×10^{13}	0	38 000	34
(78) $N + O_2 \rightarrow NO + O$	6.40×10^{9}	1.0	3 145	34
(79) $H + NO \rightarrow N + OH$	1.34×10^{14}	0	24 760	35
(80) $H + NH \rightarrow N + H_2$	1.00×10^{12}	.7	956	25
(81) $O + NH \rightarrow N + OH$	6.30×10^{11}	.5	4 026	36
(82) $O + NH \rightarrow NO + H$	6.30×10^{11}	.5	0	36
(83) $OH + NH \rightarrow N + H_2O$	5.00×10^{11}	.5	1 006	25
(84) $N_2O \rightarrow N_2 + O$	(b)			34
(85) $N_2O + CO \rightarrow N_2 + CO_2$	2.10×10^{11}	0	8 757	37
(86) $H + N_2O \rightarrow NH + NO$	1.00×10^{11}	.5	15 100	25
(87) $H + N_2O \rightarrow N_2 + OH$	7.60×10^{13}	0	7 600	34
(88) $O + N_2O \rightarrow N_2 + O_2$	1.00×10^{14}	0	14 092	34
(89) $O + N_2O \rightarrow 2NO$	1.00×10^{14}	0	14 092	34

[a]The parameters A, n, and C refer to the rate coefficient equation $k = AT^n \exp(-C/T)$. The rate coefficient units are sec^{-1} for unimolecular reactions, $cm^3/mol\text{-}sec$ for bimolecular reactions, and $cm^6/mol^2\text{-}sec$ for termolecular reactions.

[b]$k_{84} = \dfrac{1.3 \times 10^{11} \exp(-30\,000/T)}{1 + 2.6 \times 10^{-4} [M]^{-1} \exp(-1000/T)}$, where $[M]$ is the total concentration in the system.

TABLE 4.- SOME RESULTS OF PARAMETRIC STUDIES

Adjustment to mechanism	NO_x, ppm, as function of fuel-air equivalence ratio, ϕ					
	Methane (300 K)			Propane (455 K)		
	ϕ = 0.8	ϕ = 1.0	ϕ = 1.2	ϕ = 0.8	ϕ = 1.0	ϕ = 1.3
Initial mechanism	11	115	145	50	205	230
Extended Zeldovich and N_2O reactions only	3	19	0.8	22	47	2
$0.5k_{66}$ $(CH + N_2 \rightarrow HCN + N)$	6	69	83	36	117	134
$k_{59} = k_{60} = k_{61} = 0$ $(CH_2 + X \rightarrow CH + XH)$	3	19	11	36	124	132
$k_{23} = 0$ $(O + C_2H \rightarrow CO + CH)$	8	114	140	35	134	155
$10k_{25}$ $(CH + O_2 \rightarrow HCO + O)$	4	41	63	26	85	151
$50k_{62}$ $(CH + CO_2 \rightarrow HCO + CO)$	9	62	65	40	117	112
$10k_{63}$ $(CH + H \rightarrow C + H_2)$ $10k_{64}$ $(CH + OH \rightarrow C + H_2)$	5	49	101	32	93	167
Measured NO_x, ppm	10	48	50	30	74	60

1. Report No.	2. Government Accession No.	3. Recipient's Catalog No.
NASA TP-1794		

4. Title and Subtitle	5. Report Date
CHEMICAL KINETIC MODELS FOR COMBUSTION OF HYDROCARBONS AND FORMATION OF NITRIC OXIDE	December 1980
	6. Performing Organization Code 506-52-33-01
7. Author(s)	8. Performing Organization Report No.
Casimir J. Jachimowski and Charles H. Wilson	L-14106
	10. Work Unit No.
9. Performing Organization Name and Address	
NASA Langley Research Center Hampton, VA 23665	11. Contract or Grant No.
	13. Type of Report and Period Covered
12. Sponsoring Agency Name and Address	Technical Paper
National Aeronautics and Space Administration Washington, DC 20546	14. Sponsoring Agency Code

15. Supplementary Notes

16. Abstract

The formation of nitrogen oxides (NO_x) during combustion of methane, propane, and a jet fuel, JP-4, was investigated in a jet-stirred combustor. The results of the experiments were interpreted using reaction models in which the nitric oxide (NO) forming reactions were coupled to the appropriate hydrocarbon combustion reaction mechanisms. Comparison between the experimental data and the model predictions reveals that the CH + N_2 reaction process has a significant effect on NO formation especially in stoichiometric and fuel-rich mixtures. Reaction models were assembled that predicted nitric oxide levels that were in reasonable agreement with the jet-stirred combustor data and with data obtained from a high-pressure (5.9 atm (0.6 MPa)), prevaporized, premixed, flame-tube-type combustor. The results of the experiments and the theoretical studies also suggested that the behavior of hydrocarbon mixtures, like JP-4, may not be significantly different from that of pure hydrocarbons. Application of the propane combustion and nitric oxide formation model to the analysis of NO_x emission data reported for various aircraft gas turbines showed the contribution of the various nitric oxide forming processes to the total NO_x formed.

17. Key Words (Suggested by Author(s))	18. Distribution Statement
Kinetics Pollution Combustion Reaction mechanism	Unclassified - Unlimited Subject Category 25

19. Security Classif. (of this report)	20. Security Classif. (of this page)	21. No. of Pages	22. Price
Unclassified	Unclassified	29	A03

For sale by the National Technical Information Service, Springfield, Virginia 22161

NASA-Langley, 1980

END

March 2, 1981